Multiprimary Display Color Calibration: A Variational Framework for Robustness to Device Variation

Carlos Eduardo Rodríguez-Pardo, Gaurav Sharma; ECE Dept. Univ. of Rochester, Rochester, NY, USA

Abstract

For multiprimary displays, color within the interior of the gamut can be reproduced with several different control values, a situation that is in contrast with the three primary scenario, where the control values are unique. For a given color, the selection of the control values, or color calibration, becomes a fundamental step for color rendition on multiprimary devices. Because spatially smooth variations in color are common in imagery and it is critical that despite device variations these be maintained as smooth variations in renditions, it is also desirable that the calibration strategy preserve smoothness of the device control values over color space. Based on this motivation, we propose a variational framework for color calibration of multiprimary displays that emphasizes smoothness by minimizing the squared norm of the gradient of the calibration function over the display gamut. We test our proposed methodology on a four primary system, and compare its performance with calibrations obtained from other standard methodologies. Results indicate that, compared with the alternatives, the proposed variational approach offers the smoothest variation in the control values over the entire color space and as a result also exhibits enhanced robustness in the presence of device variations.

Introduction

Multiprimary displays, i.e., display systems with four or more primaries, have shown the potential to expand the gamut, and also offer flexibility that can be use to improve power consumption [1, 2], the viewing angle [3] and the resolution for rendered imagery [4].

The flexibility of multiprimary displays is a result of using more than the three primaries required for matching of human trichromatic perception. This implies that a color inside the display gamut may be reproduced using different primary combinations. However, different primary combinations that produce the same colors may have in practice an impact on other attributes of the display performance. These other attributes can guide the selection of a specific combination of primaries, or a *color calibration* as has been done in some of the afore-mentioned prior work. Smooth variations in color are common in both natural and synthetic imagery and, for maintaining naturalness, it is critical that the smoothness in such variations be preserved in renditions [5]. This becomes particularly important for the selection of the color calibration in the presence of colorimetric variations in the primaries – a criterion that is appreciated but has not thus far been formally used in multiprimary display calibration.

Strategies to introduce smoothness in the calibrations have been proposed in prior work with alternative motivations. The matrix switching algorithm [6] guarantees smoothness for luminance transitions, in particular it provides smooth transitions on the gray axis. In an extension of this work [7] proposes a methodology based on interpolations in equi-luminance planes to obtain smooth calibrations on color regions of linear transition. In [8] the center of gravity of a volume denoted as the metameric black is computed as the color control value, while [9] proposed a method based on a spherical average. In most of the cases, the smoothness of a calibration is not formally defined and, therefore, it is not explicitly optimized.

In this paper we propose a figure of merit for characterizing the smoothness of a color calibration and develop an approach for obtaining an optimal calibration under that criteria. Specifically, we formulate a variational framework for obtaining optimized calibrations for multiprimary displays that maximizes smoothness for the transition device control values over the display gamut under the presence of device variation. Our approach is shown to offer smoother transitions in the interior of the display gamut when compared to other alternatives and to also exhibit robustness in the presence of colorimetric variations in the primaries.

The manuscript is organized as follows. The first section introduces the calibrations as a function of the color space, and provides further motivation for our work. In the following section we present a mathematical analysis showing the benefits of smooth calibrations for robust color renderings. Then we introduce a figure of merit for the smoothness of calibrations based on the norm of the gradient, and a variational framework for obtaining of optimal calibrations with minimum norm of the gradient. We test our methodology and offer comparisons with other strategies in the experimental results section. Finally the conclusions section summarizes the main findings of this work.

Color Calibration Function

Consider an additive display system with K primaries, which colorimetric representation in the tristimulus coordinates in the CIE XYZ color space [10] is given by the vectors $\mathbf{p}_1, \ldots, \mathbf{p}_K$, where $\mathbf{p}_i = [p_{i,x}, p_{i,y}, p_{i,z}]^T$ are the CIE XYZ tristimulus values [10] for the i^{th} primary.

For this system the strength of the i^{th} primary is determined by a corresponding *control value* α_i, $0 \leq \alpha_i \leq 1$. Thus, the tristimulus vector $\mathbf{t} = [t_x, t_y, t_z]^T$ for the color reproduced by the display in response to the control input α, can be computed as [11–13]

$$\begin{aligned}\mathbf{t}(\alpha) &= \sum_{i=1}^{K} \alpha_i \mathbf{p}_i \\ &= \mathbf{P}\alpha,\end{aligned} \tag{1}$$

where $\mathbf{P}$ represents the $3 \times N$ primary matrix $\mathbf{P} = [\mathbf{p}_1, \mathbf{p}_2, \ldots, \mathbf{p}_K]$, and α is the primary control vector $\alpha = [\alpha_1, \alpha_2, \ldots, \alpha_K]^T$. For the rest of the document, we will assume that any selection of three

of the columns of $\mathbf{P}$ is linearly independent, which is the case for most practical systems.

In this way, $\mathbf{t}(\alpha)$ can be seen as a continuous mapping of the unitary hypercube $[0,1]^K$, also known as the *display control set*, onto the colorimetric space CIE XYZ defined by the matrix $\mathbf{P}$. The image of such mapping is the the *display gamut* $\mathscr{G}$, which is the set of colors that the device can reproduce and can be defined as

$$\mathscr{G} = \left\{\mathbf{t} = \mathbf{P}\alpha | \alpha \in [0,1]^K\right\}. \quad (2)$$

In order to reproduce a color, the inverse relationship to the model presented in equation (1) is required. That is, for a given color $\mathbf{t}$ to be reproduced, it is needed to determine the adequate primary control vector α that drives the display to reproduce $\mathbf{t}$. Note that in the three primary scenario, $\mathbf{P}$ is a non-singular 3×3 matrix, and therefore, the relationship between $\mathbf{t}$ and α is uniquely determined by the primary matrix, and the inverse model can be expressed as, $\alpha = \mathbf{P}^{-1}\mathbf{t}$.

In a multiprimary display, however, the system of equations (1) is under-determined, and therefore, multiple control values α may be found to reproduce a color $\mathbf{t}$. A particular choice of a control vector is referred in this paper as a *calibration* for tristimulus $\mathbf{t}$. In [14], we presented a complete characterization for the set of possible calibrations for the tristimulus $\mathbf{t}$, which we refer to as the *calibration set* of $\mathbf{t}$ and denoted by $\Omega(\mathbf{t})$. As also demonstrated in [14] the characterization of the calibration set $\Omega(\mathbf{t})$ can be exploited for the selection of a calibration with specific desirable properties.

In practice, because smooth variations are common in rendered imagery and need to be maintained in the presence of device and observer variation, it is important to consider not only the calibration for each color, but also to consider the transition of calibrations through the space of color. A *calibration function* $\alpha(\mathbf{t}) : \mathscr{G} \rightarrow [0,1]^k$, can be defined on the display gamut $\mathscr{G}$ by selecting for each tristimulus $\mathbf{t}$ one of the possible calibration vectors.

To provide an example, consider the display defined by the primaries [15]

$$\mathbf{P} = [\mathbf{p}_1, \mathbf{p}_2, \mathbf{p}_3, \mathbf{p}_4] \stackrel{\text{def}}{=} \begin{bmatrix} 0.3630 & 0.1539 & 0.0471 & 0.0758 \\ 0.1761 & 0.3700 & 0.3093 & 0.0244 \\ 0.0027 & 0.0179 & 0.1853 & 0.4415 \end{bmatrix}, \quad (3)$$

and a calibration function $\alpha_{random}(\mathbf{t})$ defined by choosing for each each color a random vector from the set of possible calibrations that satisfy (1). Consider in particular calibration values for the gray axis ramp (a ramp with colors varying on luminance (L^*) and with zero chromatic components (u^*, v^*) in the CIE LUV space).

Though the calibration function $\alpha_{random}(\mathbf{t})$ is not a continuous function, in the ideal setting, smooth transitions in requested colors $\mathbf{t}$ are rendered accurately preserving both the color and the smoothness of the transitions. However, in the presence of device variations this ideal behavior is compromised. Consider the Fig. 1(a) that shows image patches of corresponding to a gray ramp (a sampling along the L^* axis) in the ideal setting, where $\alpha_{random}(\mathbf{t})$ or any other calibration function may be utilized. However, when the display is perturbed by varying one of the primaries by adding noise equivalent to 40% its magnitude[1], the random variations in $\alpha_{random}(\mathbf{t})$ map into perceptible random variations in the hues of the patches and appear quite objectionable, as is shown in Fig. 1(b). Smoothness of the calibration function $\alpha(\mathbf{t})$ along smooth trajectories of the desired color $\mathbf{t}$ in color space is therefore a desirable property. We develop a formal metric for smoothness and a framework for optimizing the metric. Before doing so, we introduce a methodology for visualizing multiprimary display calibrations that allows us to better illustrate the smoothness of, or lack thereof, in different calibration functions.

(a) Rendering by original system

(b) Perturbed system, random calibration α_{random}

Figure 1: Gray axis rendering by a random calibration α_{random} under primary variation. **To appreciate the color differences, please see the electronic version of the document**.

Visualization of Calibration Functions

The calibration functions for multiprimary systems are functions of more than three variables and consequently cannot be directly visualized. For multiprimary systems with $K = 4, 5$, and 6 primaries, however, a visual representation is still possible based on a subspace decomposition of the display control space that we proposed in [14]. In this decomposition a calibration $\alpha(\mathbf{t})$ for color $\mathbf{t}$ can be decomposed in terms of a 3 dimensional *control visual subspace* (CVS), which is determined completely by the color $\mathbf{t}$, and a $(K-3)$ dimensional *control black space* (CBS) that contains the differences between all alternative calibrations for $\mathbf{t}$, and therefore it is in this subspace that meaningful comparisons between calibrations can be done. If $\mathbf{B}$ represents a $K\times(K-3)$ matrix which columns contains a basis for CBS, then the calibration vector α for color $\mathbf{t}$ can be expressed as

$$\begin{aligned}\alpha &= \mathbf{P}^T\left(\mathbf{P}\mathbf{P}^T\right)^{-1}\mathbf{t} + \mathbf{B}\mathbf{B}^T\alpha \\ &= \mathbf{P}^T\left(\mathbf{P}\mathbf{P}^T\right)^{-1}\mathbf{t} + \mathbf{B}\beta, \end{aligned} \quad (4)$$

where $\beta = \mathbf{B}^T\alpha$ is the $(K-3)$ vector that represents the CBS component of α, which can be visualized for systems with $K = 4, 5$, and 6 primaries in $1, 2$, and 3 dimensions, respectively. In the same way, the calibration set for $\mathbf{t}$, $\Omega(\mathbf{t})$ can also be decomposed as

$$\Omega(\mathbf{t}) = \mathbf{P}^T\left(\mathbf{P}\mathbf{P}^T\right)^{-1}\mathbf{t} + \mathbf{B}\Xi(\mathbf{t}), \quad (5)$$

where $\Xi(\mathbf{t}) = \mathbf{B}^T\Omega(\mathbf{t})$ is a set that lies entirely on CBS. Additional details on the definition the subspace decomposition can be found in [14].

As an example let consider the system and the calibration function $\alpha_{random}(\mathbf{t})$ introduced in the last section. For this case

[1] The relatively large perturbation is chosen to ensure that the effects can be seen despite other sources of variation encountered in the reproduction process.

the CBS is a one dimensional subspace, and therefore $\beta(\mathbf{t}) = \mathbf{B}^T \alpha_{random}(\mathbf{t})$ is a scalar function. Consider in particular calibration values for the gray axis ramp (a ramp with colors varying on luminance (L^*) and with zero chromatic components (u^*, v^*) in the CIE LUV space). In Fig. 2 the green line represents the function $\beta(\mathbf{t})$, when the ramp varies from black ($L^* = 0$) to white ($L^* = 100$). For each luminance value an additional black line is shown, which represents $\Xi(\mathbf{t})$, the CBS components of the calibration set for color $\mathbf{t}$, giving the intuition of how different calibrations functions can be considered to reproduce the same ramp. Note that for the colors black and white, the calibration set is one single point which means that the calibration is unique. This is true for all colors on the surface of the gamut [16].

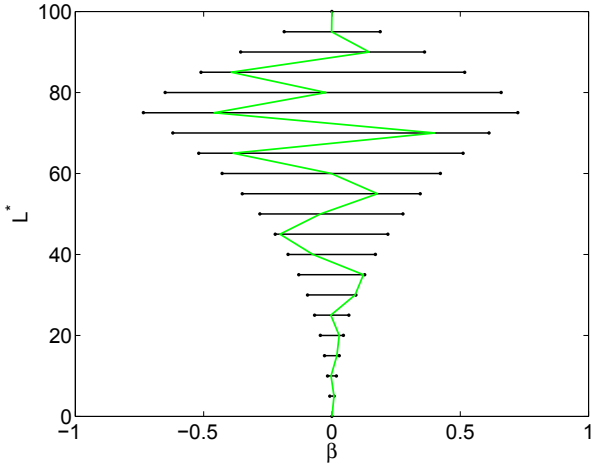

Figure 2: A representation for the calibration $\alpha_{random}(\mathbf{t})$ on the gray ramp with values $(L*, 0, 0)$ in the CIE LUV color space. The horizontal axis shows the variation of luminance, while the vertical one shows the values of $\beta(\mathbf{t})$, the projection of $\alpha_{random}(\mathbf{t})$ on the CBS.

Robust Calibration

Suppose that a display system defined by the matrix $\mathbf{P}$ is perturbed by changing the primaries by the perturbation (matrix) $\Delta\mathbf{P}$. Instead of reproducing a color $\mathbf{t}$, the new system, reproduces a color $\hat{\mathbf{t}}$,

$$\begin{aligned}\hat{\mathbf{t}}(\mathbf{t}) &= (\mathbf{P}+\Delta\mathbf{P})\,\alpha(\mathbf{t}) \\ &= \mathbf{t}+\Delta\mathbf{P}\alpha(\mathbf{t}),\end{aligned} \tag{6}$$

where the dependency of $\hat{\mathbf{t}}$ on the variable $\mathbf{t}$ expressed in equation (6), although awkward at first glance, makes explicit the fact that the calibration vector was intended to reproduce $\mathbf{t}$.

The perturbation not only affects the accuracy of the color reproduction but also its smoothness. As seen in Fig. 1, under the presence of device variations, the non-smooth variations of a calibration function $\alpha(\mathbf{t})$ would be rendered visible and objectionable as non-smooth variations of color. To minimize that effect, we are interested in finding calibration functions that best preserve the smoothness in the transitions of color.

Given a tristimulus $\mathbf{t}$, we are interested in evaluating the effect of primary perturbation on the rendering of the pair of colors $\mathbf{t}$ and $\mathbf{t}+\Delta\mathbf{t}$, for certain color difference $\Delta\mathbf{t}$. For simplicity in the analysis, we consider color differences along the direction of a given unitary vector $\mathbf{u}$, that is $\Delta\mathbf{t}(s\mathbf{u}) = s\mathbf{u}$, where s is a scalar. An ideal rendering for this color pair using any calibration function α preserves the color difference $\Delta\mathbf{t}(s\mathbf{u})$, while the color difference between the corresponding renderings by the perturbed system, denoted by $\Delta\hat{\mathbf{t}}(s\mathbf{u})$, is

$$\begin{aligned}\Delta\hat{\mathbf{t}}(s\mathbf{u}) &= \hat{\mathbf{t}}(\mathbf{t}+s\mathbf{u}) - \hat{\mathbf{t}}(\mathbf{t}) \\ &= s\mathbf{u} + \Delta\mathbf{P}\left[\alpha(\mathbf{t}+s\mathbf{u}) - \alpha(\mathbf{t})\right] \\ &= \Delta\mathbf{t}(s\mathbf{u}) + \Delta\mathbf{P}\left[\alpha(\mathbf{t}+s\mathbf{u}) - \alpha(\mathbf{t})\right].\end{aligned} \tag{7}$$

In this way the tristimulus difference between colors rendered by the perturbed system depends on the primary perturbation $\Delta\mathbf{P}$, which cannot be controlled in practice, and the calibration function $\alpha(\mathbf{t})$, which can be suitably designed. In this context, we assume that the calibration functions $\alpha(\mathbf{t})$ that we consider are differentiable with continuous derivatives everywhere inside the gamut. We then define the deviation at color $\mathbf{t}$ in the direction $\mathbf{u}$, as the directional derivative

$$\begin{aligned}\delta(\mathbf{t},\mathbf{u}) &\equiv \lim_{s\to 0} \frac{\Delta\hat{\mathbf{t}}(s\mathbf{u}) - \Delta\mathbf{t}(s\mathbf{u})}{s} \\ &= \Delta\mathbf{P} \lim_{s\to 0} \frac{\alpha(\mathbf{t}+s\mathbf{u}) - \alpha(\mathbf{t})}{s} \\ &= \Delta\mathbf{P}\mathbf{d}(\mathbf{t},\mathbf{u}),\end{aligned} \tag{8}$$

where $\mathbf{d}(\mathbf{t},\mathbf{u})$ is the $K \times 1$ vector which k^{th} component is given by the Gateaux directional derivative [17] of $\alpha_k(\mathbf{t})$ in direction $\mathbf{u}$, that is,

$$[\mathbf{d}(\mathbf{t},\mathbf{u})]_k \equiv \lim_{s\to 0} \frac{\alpha_k(\mathbf{t}+s\mathbf{u}) - \alpha_k(\mathbf{t})}{s}. \tag{9}$$

The deviation function $\delta(\mathbf{t},\mathbf{u})$ provides an indication for robustness of color reproduction: A rendering with low deviation preserves the color differences better than a rendering with a higher deviation.

Although $\delta(\mathbf{t},\mathbf{u})$ is defined for an specific direction in the transition of colors, the norm of this vector can be bounded for any direction as the following lemma sates, whose proof is provided in the appendix.

Lemma 1 *For a display system* $\mathbf{P}$ *perturbed by matrix* $\Delta\mathbf{P}$*, there exists a constant* $C_{\Delta\mathbf{P}} > 0$ *such that for all unitary* 3×1 *vector* $\mathbf{u}$*, the deviation for color* $\mathbf{t}$*,* $\delta(\mathbf{t},\mathbf{u})$ *is bounded as,*

$$\|\delta(\mathbf{t},\mathbf{u})\|^2 \le C_{\Delta\mathbf{P}} \sum_{k=1}^{K} \|\nabla\alpha_k(\mathbf{t})\|^2, \tag{10}$$

where $\nabla\alpha_k(\mathbf{t})$ *is the gradient of the* k^{th} *component of the calibration function.*

Thus the deviation $\delta(\mathbf{t},\mathbf{u})$ is bounded by the scalar constant $C_{\Delta\mathbf{P}}$, which depends exclusively on the perturbation and can not be controlled, and a term that involves the norm of the gradients. Therefore, the effect of device variation can be mitigated by selecting smooth calibration functions with minimum gradient norm. A strategy for optimal computation of such functions is established under a variational framework in the following section.

Variational Formulation

For a given multiprimary system with primaries tristimulus $\mathbf{p}_1, \mathbf{p}_2, \ldots, \mathbf{p}_K$, and a calibration function $\alpha(\mathbf{t}) = [\alpha_1(\mathbf{t}), \alpha_2(\mathbf{t}), \ldots, \alpha_K(\mathbf{t})]^T$ defined for each color vector $\mathbf{t}$ in the display gamut $\mathscr{G}$, we define the functional $\Theta(\alpha)$,

$$\Theta(\alpha) = \int_{\mathscr{G}} \sum_{k=1}^{K} \|\nabla \alpha_k(\mathbf{t})\|^2 \, d\mathbf{t}, \tag{11}$$

and propose it as a figure of merit for the smoothness of the calibration $\alpha(\mathbf{t})$. The optimal calibration under this criteria is a function $\alpha_\Theta(\mathbf{t})$ that solves the following optimization problem

$$\begin{aligned} &\min \int_{\mathscr{G}} \sum_{k=1}^{K} \|\nabla \alpha_k(\mathbf{t})\|^2 \, d\mathbf{t}, \\ &\text{s.t. } \mathbf{P}\alpha(\mathbf{t}) = \mathbf{t}, \text{ and,} \\ &\quad 0 \le \alpha_k(\mathbf{t}) \le 1, \text{ for } k = 1, \ldots, K, \text{ for all } \mathbf{t} \in \mathscr{G}. \end{aligned} \tag{12}$$

The linear constraints in (12) express the condition that the function at each $\mathbf{t}$ belongs to the calibrations set $\Omega(\mathbf{t})$, and in this way the problem can be expressed equivalently as follows,

$$\begin{aligned} &\min \Theta(\alpha), \\ &\text{s.t. } \alpha(\mathbf{t}) \in \Omega(\mathbf{t}), \text{ for all } \mathbf{t} \in \mathscr{G}, \end{aligned} \tag{13}$$

a formulation that allows us to explicitly use the convexity properties of calibration set [14] to propose a projected gradient descend scheme based on the the calculus of variations [18], and a numerical discretization.

We first define the projection operator $\mathscr{P}_\mathbf{t}(\alpha) : \mathbb{R}^K \to \Omega(\mathbf{t})$

$$\mathscr{P}_\mathbf{t}(\alpha) = \underset{\beta \in \Omega(\mathbf{t})}{\arg\min} \|\beta - \alpha\|, \tag{14}$$

which is a well defined operator given the convexity of $\Omega(\mathbf{t})$. We then formulate the projected gradient descent algorithm [19, 20] in the following way,

$$\alpha^{n+1}(\mathbf{t}) = \mathscr{P}_\mathbf{t}(\alpha^n(\mathbf{t}) - \eta \nabla_\alpha \Theta(\alpha(\mathbf{t}))) \tag{15}$$

where n represents the iteration, η is the step size of the descent, and $\nabla_\alpha \Theta$ is the $K \times 1$ vector of variational derivatives of Θ with respect $\alpha_k(\mathbf{t})$, $k = 1, \ldots, K$, and which k^{th} component ∇_{α_k}, is defined as

$$\begin{aligned} \nabla_{\alpha_k} \Theta = &\frac{\partial}{\partial \alpha_k} \left(\sum_{k=1}^{K} \|\nabla \alpha_k(\mathbf{t})\|^2 \right) \\ &- \sum_{j=1}^{3} \frac{\partial}{\partial t_j} \frac{\partial}{\partial \alpha'_{k,t_j}} \left(\sum_{k=1}^{K} \|\nabla \alpha_k(\mathbf{t})\|^2 \right), \end{aligned} \tag{16}$$

where $\alpha'_{k,t_j} = \frac{\partial}{\partial t_j} \alpha_k(\mathbf{t})$. It can be shown that the expression in (16) can be simplified to

$$\nabla_{\alpha_k} \Theta = -2 \sum_{j=1}^{3} \frac{\partial^2}{\partial t_j^2} \alpha_k(\mathbf{t}). \tag{17}$$

Results

We tested our methodology on a four primary system, and compared it with other methodologies including matrix switching $\alpha_{MS}(\mathbf{t})$ [6], minimum optical power, $\alpha_{mOP}(\mathbf{t})$ [14, 21, 22], maximum optical power $\alpha_{MOP}(\mathbf{t})$ [14], the random calibration $\alpha_{random}(\mathbf{t})$, and the mean calibration $\alpha_{mc}(\mathbf{t})$ [14], that for the four primary case also corresponds to strategy proposed in [8]. The optimal calibration function $\alpha_\Theta(\mathbf{t})$ for our method is obtained by discretizing the calibration function over a uniform grid of points covering the entire display gamut $\mathscr{G}$ and using the gradient descent algorithm in (15) to numerically perform the minimization.

For each of the considered strategies we computed the display renderings they offer under device variation, by using the primaries in (3) and perturbing one of the primaries of the system by a vector equivalent to 40% of its magnitude. We then compare the impact of the perturbation on the different calibration functions by comparing the renderings for a limited number of trajectories in color space for the ideal non-perturbed system for which all the calibration functions provide the same results and for each of the calibration functions for the perturbed system. Also, using the visualization methodology proposed in [14], we compare the different calibration functions for the chosen trajectories to illustrate the extent of variation that each encounters within the control black space.

As a first trajectory in color space, we consider the gray ramp for which the rendered results are shown in Fig. 3, where it can be appreciated that the proposed methodology, the matrix switching strategy and the mean calibration are able to offer renderings that preserve the smoothness of the gray ramp, in contrast to the rendering obtained from the random calibration shown in Fig. 3(b). In the presence of the perturbation, the power optimal calibrations also show clearly visible and objectionable variations in hue.

Figure 4 shows the results for a second trajectory inside the color gamut consisting of a sweep obtained by varying the v^* component, with constant values $u^* = 20, L^* = 60$. In this case, from Fig. 4 it can be appreciated that the proposed methodology (α_Θ) offers color transitions that best match the smoothness of the original ramp. The other strategies offer renderings with noticeable sharp transitions over the ramp exhibited visually as contouring artifacts. The relative values for $\Theta(\alpha)$ for the different strategies are shown in Table 1.

Figure 5 shows a representation of the calibrations functions for the different methodologies in the control black space for our two chosen smooth trajectories in color space. Each of the horizontal lines is a representation of the calibration set for a corresponding color in the color ramp/sweep (the set of all possible feasible calibrations for the color), and the colored lines on top are the calibration functions. The subfigures correspond to the two chosen trajectories: Fig.5(a) to the gray ramp and Fig.5(b) to the v^* sweep. For the gray ramp (Fig.5(a)), the optimal power calibrations take values at the extremes of the calibration sets, varying considerably, while the proposed scheme, matrix switching, and mean calibration, offer the same calibration function, the smoothest function possible for this case. For the v^* sweep (Fig.5(b)), the matrix switching and mean calibration schemes provide calibrations with sharp changes, whereas the proposed methodology (α_Θ) offers the smoothest calibration among the considered strategies. Similar behavior can be seen for the different calibration functions over other smooth trajectories through

Calibration	$\Theta(\alpha)/\Theta(\alpha_\Theta)$
$\alpha_\Theta(\mathbf{t})$	1
$\alpha_{MS}(\mathbf{t})$	1.10
$\alpha_{mc}(\mathbf{t})$	1.43
$\alpha_{mOP}(\mathbf{t})$	1.78
$\alpha_{MOP}(\mathbf{t})$	1.75

Table 1: Normalized gradient variation over the gamut $\Theta(\alpha)/\Theta(\alpha_\Theta)$ for the different calibration functions.

the display gamut.

In the presence of the perturbations simulating device variation, the calibrations obtained with each of the prior heuristic methodologies all show undesirable variations through the color space ($\alpha_{random}(\mathbf{t})$, $\alpha_{mOP}(\mathbf{t})$, and,$\alpha_{MOP}(\mathbf{t})$), or in regions outside the limited axis for which they are optimized ($\alpha_{MS}(\mathbf{t}), \alpha_{mc}(\mathbf{t})$). The proposed calibration methodology on the other hand, because of its smoothness through the display gamut (see Fig. 5) exhibits much better behavior under the device variations (perturbations).

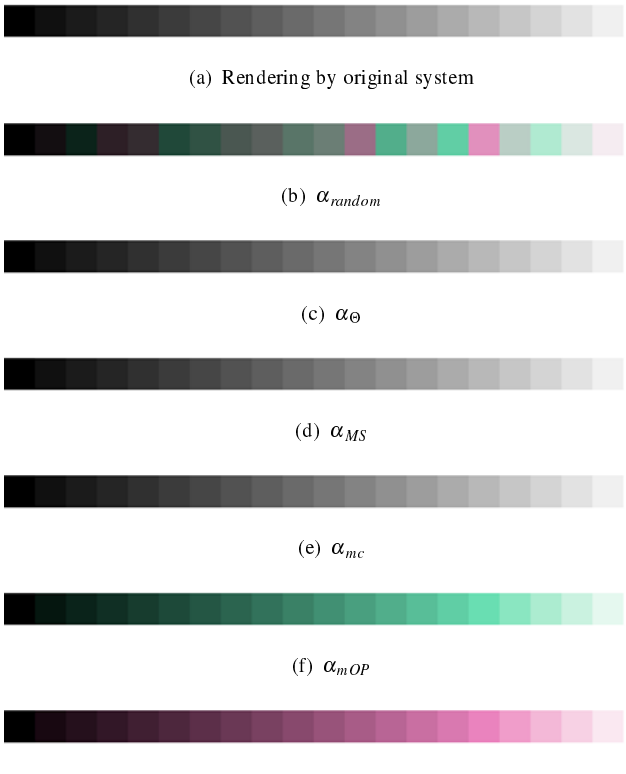

(a) Rendering by original system

(b) α_{random}

(c) α_Θ

(d) α_{MS}

(e) α_{mc}

(f) α_{mOP}

(g) α_{MOP}

Figure 3: Rendering of the gray ramp by a four primary display system. On the top, the reproduction by the original display, followed by the renderings of the perturbed system using different calibration strategies: A random calibration $\alpha_{random}(\mathbf{t})$, our methodology $\alpha_\Theta(\mathbf{t})$, matrix switching $\alpha_{MS}(\mathbf{t})$ [6], mean calibration $\alpha_{mc}(\mathbf{t})$ [8, 14], minimum optical power, $\alpha_{mOP}(\mathbf{t})$ [14, 21, 22], and maximum optical power $\alpha_{MOP}(\mathbf{t})$ [14]. **To appreciate the color differences, please see the electronic version of the document**.

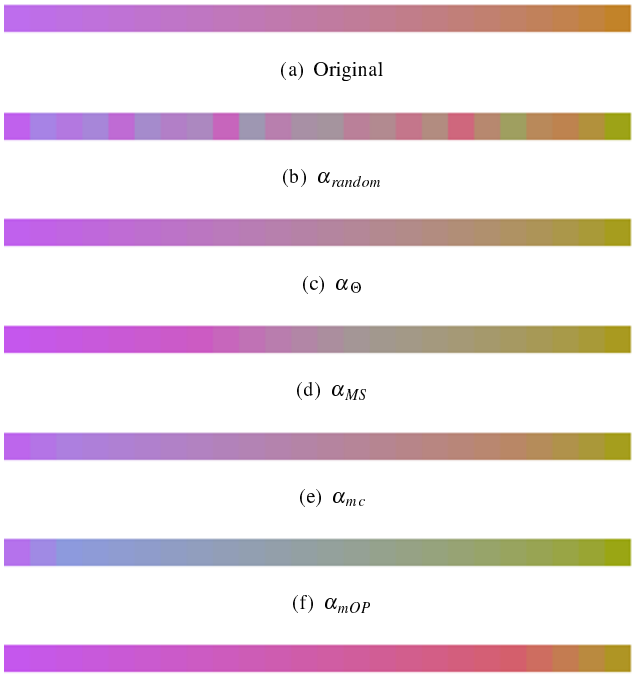

(a) Original

(b) α_{random}

(c) α_Θ

(d) α_{MS}

(e) α_{mc}

(f) α_{mOP}

(g) α_{MOP}

Figure 4: Rendering of the ramp obtained by varying the v^* component, with constant values $u^* = 20, L^* = 60$ by a four primary display system. On the top, the reproduction by the original display, followed by the renderings of the perturbed system using different calibration strategies: A random calibration $\alpha_{random}(\mathbf{t})$, our methodology $\alpha_\Theta(\mathbf{t})$, matrix switching $\alpha_{MS}(\mathbf{t})$ [6], mean calibration $\alpha_{mc}(\mathbf{t})$ [8, 14], minimum optical power, $\alpha_{mOP}(\mathbf{t})$ [14, 21, 22], and maximum optical power $\alpha_{MOP}(\mathbf{t})$ [14]. **To appreciate the color differences, please see the electronic version of the document**.

Conclusion and Discussion

We provided an analysis for robustness of color reproduction that shows the relationship between robustness and smoothness of calibration functions often seen in practice. Our framework provides the first mathematical formulation for quantitative evaluation and optimization of smoothness of color calibrations functions for multiprimary displays. The optimized calibrations obtained from this methodology offer the smoothest variation in the control values over the entire gamut, as compared with calibrations obtained from other standard strategies, showing enhanced robustness in the presence of device variation.

Appendix

The following is a proof for lemma 1.

From Equation (8) the squared norm of the deviation on a given tristimulus $\mathbf{t}$ is

$$\|\delta(\mathbf{t},\mathbf{u})\|^2 = \|\Delta\mathbf{P}\mathbf{d}(s\mathbf{u})\|^2 . \tag{18}$$

Now define $C_{\Delta\mathbf{P}}$ as the matrix $2-$norm of $\Delta\mathbf{P}$,

$$C^2_{\Delta\mathbf{P}} = \sup_{\substack{\mathbf{v}\in\mathbb{R}^k \\ \|\mathbf{v}\|\neq 0}} \frac{\|\Delta\mathbf{P}\mathbf{v}\|^2}{\|\mathbf{v}\|^2}, \tag{19}$$

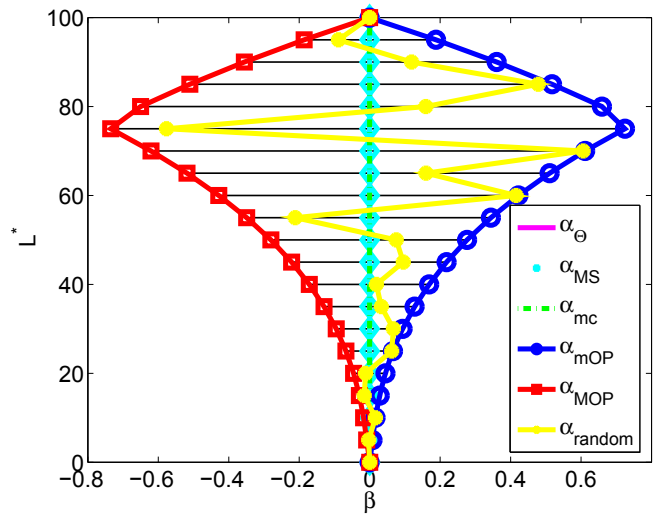

(a) Gray axis, $u^* = v^* = 0$

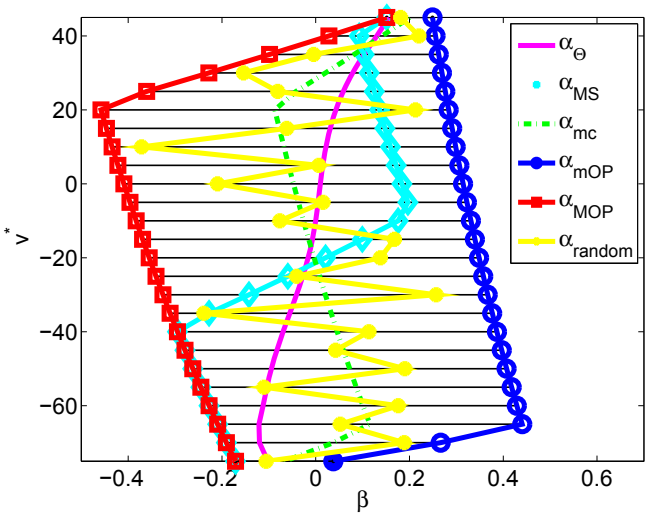

(b) v^* ramp, $u^* = 20, L^* = 60$

Figure 5: Visualization of the calibration functions on different regions of the gamut obtained from different strategies: A random calibration $\alpha_{random}(\mathbf{t})$, our methodology $\alpha_{\Theta}(\mathbf{t})$, matrix switching $\alpha_{MS}(\mathbf{t})$ [6], mean calibration $\alpha_{mc}(\mathbf{t})$ [8, 14], minimum optical power, $\alpha_{mOP}(\mathbf{t})$ [14, 21, 22], and maximum optical power $\alpha_{MOP}(\mathbf{t})$ [14].

Because $\alpha(\mathbf{t})$ is different for different values of $\mathbf{t}$, the limit in equation (9) is nonzero, $\|\delta(\mathbf{t},\mathbf{u})\|^2 > 0$ for all $\mathbf{t}$ and $\mathbf{u}$, we have that

$$\|\delta(\mathbf{t},\mathbf{u})\|^2 = \|\Delta\mathbf{P}\mathbf{d}(s\mathbf{u})\|^2 \frac{\|\mathbf{d}(s\mathbf{u})\|^2}{\|\mathbf{d}(s\mathbf{u})\|^2} \leq C_{\Delta\mathbf{P}}^2 \|\mathbf{d}(s\mathbf{u})\|^2 . \quad (20)$$

Since the directional derivative can be expressed in terms of the gradient as $[\mathbf{d}(\mathbf{t},\mathbf{u})]_k = \nabla\alpha_k(\mathbf{t}) \cdot \mathbf{u}$ [23, pp.147], thus

$$\|\delta(\mathbf{t},\mathbf{u})\|^2 \leq C_{\Delta\mathbf{P}}^2 \sum_{k=1}^{K} (\nabla\alpha_k(\mathbf{t}) \cdot \mathbf{u})^2 , \quad (21)$$

Now, setting $\mathbf{u} = \frac{\nabla\alpha_k(\mathbf{t})}{\|\nabla\alpha_k(\mathbf{t})\|}$ we obtain the desired result

$$\|\delta(\mathbf{t},\mathbf{u})\|^2 \leq C_{\Delta\mathbf{P}}^2 \sum_{k=1}^{K} \left(\nabla\alpha_k(\mathbf{t}) \cdot \frac{\nabla\alpha_k(\mathbf{t})}{\|\nabla\alpha_k(\mathbf{t})\|}\right)^2 = C_{\Delta\mathbf{P}}^2 \sum_{k=1}^{K} \|\nabla\alpha_k(\mathbf{t})\|^2 . \quad (22)$$

∎

References

[1] K. Yoshiyama, M. Teragawa, A. Yoshida, K. Tomizawa, K. Nakamura, Y. Yoshida, and Y. Yamamoto, "Power-saving: A new advantage of multi-primary color displays derived by numerical analysis," in *SID Symposium Digest of Technical Papers*, vol. 41, May 2010, pp. 416–418.

[2] C.-C. Tsai, F.-C. Lin, Y.-P. Huang, , and H.-P. D. Shieh, "RGBW 4-in-1 LEDs for backlight system for ultra-low power consumption field-sequential-color LCDs," in *SID Symposium Digest of Technical Papers*, vol. 41, May 2010, pp. 420–423.

[3] S. Ueki, K. Nakamura, Yuhichi, Yoshida, T. Mori, K. Tomizawa, Y. Narutaki, Y. Itoh, , and K. Okamoto, "Five-Primary-Color 60-inch LCD with novel wide color gamut and wide viewing angle," in *SID Symposium Digest of Technical Papers*, vol. 40, June 2009, pp. 927–930.

[4] M. Teragawa, A. Yoshida, K. Yoshiyama, S. Nakagawa, K. Tomizawa, and Y. Yoshida, "Review paper: Multi-primary-color displays: The latest technologies and their benefits," *Journal of the Society for Information Display*, vol. 20, no. 1, pp. 1–11, 2012.

[5] T. Olson, "Smooth ramps: Walking the straight and narrow path through color space," in *Proc. IS&T/SID Seventh Color Imaging Conference: Color Science, Systems and Applications*, Scottsdale, AZ, 16-19 Nov. 1999, pp. 57–64.

[6] T. Ajito, K. Ohsawa, T. Obi, M. Yamaguchi, and N. Ohyama, "Color conversion method for multiprimary display using matrix switching," *Optical Review*, vol. 8, no. 2, pp. 191–197, 2001.

[7] H. Motomura, "Color conversion for a multi-primary display using linear interpolation on equi-luminance plane method (liquid)," *Journal of the Society for Information Display*, vol. 11, no. 2, pp. 371–378, 2003.

[8] F. Konig, K. Ohsawa, M. Yamaguchia, N. Ohyama, and B. Hill, "A multiprimary display: Optimized control values for displaying tristimulus values," in *Proc. IS&T/SID*

PICS 2002: Image Processing, Image Quality, Image Capture Systems Conference. Society for Imaging Science & Technology, 2002, pp. 215–220.

[9] H. Kanazawa, M. Mitsui, M. Yamaguchi, H. Haneishi, and N. Ohyama, "Color conversion for multi-primary displays using a spherical average method," in *Color and Imaging Conference*, vol. 2004, no. 1. Society for Imaging Science and Technology, 2004, pp. 65–69.

[10] CIE, "Colorimetry," CIE Publication No. 15.2, Central Bureau of the CIE, Vienna, 1986, the commonly used data on color matching functions is available at the CIE web site at http://www.cie.co.at/.

[11] G. Sharma and H. J. Trussell, "Digital color imaging," *IEEE Trans. Image Proc.*, vol. 6, no. 7, pp. 901–932, Jul. 1997.

[12] G. Sharma, "LCDs versus CRTs: Color-calibration and gamut considerations," *Proc. IEEE*, vol. 90, no. 4, pp. 605–622, Apr. 2002.

[13] M. J. Vrhel and H. J. Trussell, "Color device calibration: A mathematical formulation," *IEEE Trans. Image Proc.*, vol. 8, no. 12, pp. 1796–1806, Dec. 1999.

[14] C. E. Rodríguez-Pardo and G. Sharma, "Calibration sets for multiprimary displays: Representation, visualization, and applications," in *Proc. IS&T/SID 22nd Color and Imaging Conference*, Boston, MA, 3-7 Nov. 2014, pp. 171–179.

[15] S. Wen, "Design of relative primary luminances for four-primary displays," *Displays*, vol. 26, no. 4-5, pp. 171 – 176, 2005.

[16] P. Centore, "Non-metamerism of boundary colors in multi-primary displays," *Journal of the Society for Information Display*, vol. 20, no. 4, pp. 214–220, 2012.

[17] V. Tikhomirov, "Gâteaux variation," in *Encyclopedia of Mathematics*, M. Hazewinkel, Ed. Springer, 2001.

[18] I. Gelfand and S. Fomin, *Calculus of variations. Revised English edition translated and edited by Richard A. Silverman*. Prentice-Hall Inc., Englewood Cliffs, NJ, 1963.

[19] A. A. Goldstein *et al.*, "Convex programming in hilbert space," *Bulletin of the American Mathematical Society*, vol. 70, no. 5, pp. 709–710, 1964.

[20] P. H. Calamai and J. J. Moré, "Projected gradient methods for linearly constrained problems," *Mathematical programming*, vol. 39, no. 1, pp. 93–116, 1987.

[21] M. Takaya, K. Ito, G. Ohashi, and Y. Shimodaira, "Color-conversion method for a multi-primary display to reduce power consumption and conversion time," *Journal of the Society for Information Display*, vol. 13, no. 8, pp. 685–690, 2012.

[22] P. Centore, "Minimal-energy control sequences for linear multi-primary displays," *Journal of Imaging Science and Technology*, vol. 59, no. 5, pp. 50 502–1, 2015.

[23] J. E. Marsden and A. Tromba, *Vector calculus*. W.H. Freedman and Company, 1988.